Optimization of a Switching Strategy for a Synchronous Motor Fed by a Current Inverter Using Finite Element Analysis

Vasile Manoliu

POLITEHNICA University of Bucharest, Electrical Engineering Faculty, Splaiul Independentei 313, 060042, Bucharest, Romania, vasilem@amotion.pub.ro

In a load-commutated synchronous motor, the torque is driven by the currents in the stator windings, and these currents depend on the rotor position. Since the stator phases are star-connected, the static torque generated by two stator phases connected in series and powered with a constant current offers sufficient information to design a suitable current control strategy. The synchronous machine studied has a reverse type of construction. The switching sequence for the current inverter is correlated with the rotor position by magnetostatic simulation in FLUX2D, using the maximization of static torque as optimization criteria. This study also covers a computational method for determining the operating parameters of a synchronous machine using simulation of the Standstill Frequency Response Test (SSFR).
Keywords synchronous machine, finite element, static torque, optimization.

1 Introduction

A synchronous machine with reverse type of construction has three identical phase-windings spaced around the internal periphery of the rotor magnetic core with a geometrical angle of $2\pi/3p$ between them (where p is the number of pole pairs). The rotor core is made of electrical-steel laminations, electrically insulated and slotted. The stator magnetic core (either with salient or non-salient poles) contains a d.c. (direct current) excitation winding.
The Park-Blondel equations are much used in studying the dynamic operation of a synchronous motor. In this reference system, the axis of a North pole of the stator is called the direct axis (denoted d) and the leading axis (with respect to the direction of the speed Ω) is called quadrature axis (denoted q).
In this paper a load-commutated synchronous machine model is studied. This model takes into account both the magnetic circuit configuration of the machine and the realistic construction of the damper winding.
These machines are robust and have a good weight/size to power ratio. Compared to a conventional brushed d.c. motor in which commutation is handled by carbon or copper brushes, the load-commutated synchronous motor commutation is controlled by electronics. In Fig.1 a schematic layout of the synchronous motor fed by current inverter is presented.

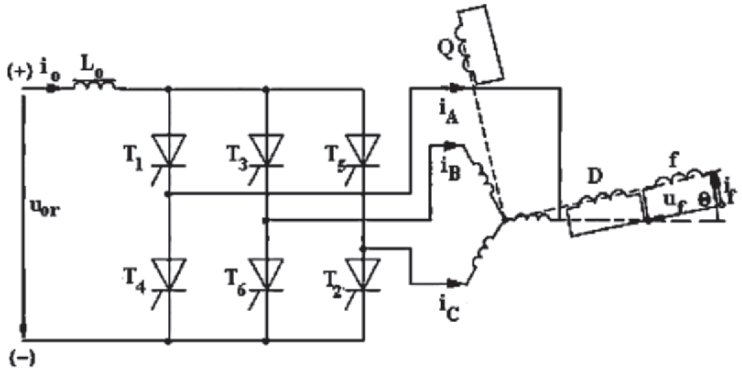

Fig. 1: Synchronous motor fed by a current inverter

An electronic supply by time-shaped rectangular currents uses a very simple and cheap rotor position sensor. The position of the rotor is needed to determine a proper timing of commutation.
Moreover, in using this kind of supply, the choice of a fractional number of slots per pole and phase ensures low torque ripple.
For this kind of synchronous motors, the drive of air compressors is an interesting application. In this case, since the starting (load) torque is very high, by replacing the asynchronous motor with a synchronous motor, the operating proves to be more economical.
Controlling without a position sensor is possible if the back electromotive force (emf) is measured; this control is recommended for applications where high starting torque is not required.
Since for the load-commutated synchronous motor the electromagnetic torque is affected by the back emf and the rotor (armature) currents, it is important to have a thorough knowledge of the static torques for designing a suitable current control strategy. For this reason, the static torque can be measured by connecting two rotor phases in series, using a constant current as source.
At the same time, the motor parameters affect the switching control. The useful characteristic parameters appear in equivalent circuits associated with the direct-axis and quadrature-axis of the synchronous machine.
By the FLUX 2D [FLU05] program 2D FEM field calculations can be made to determine these parameters as well as the static torque. This program offers a lot of useful features like partially automatic mesh generation, sliding air gap band for calculations in rotation, and external coupling circuits.
For determining the operating parameters of a synchronous machine, the simulation of the Standstill Frequency Response Test (SSFR) was used.
This approach can be used not only for the verification of the important characteristic quantities of an existing machine, but also allows optimization in designing a new machine.

2 Methods

The current supply of synchronous machine consists in imposing current amplitude in the machine windings and its phase with respect to the electromotive force E. To detect the phase angle of the electromotive force (leading angle) x_0, a rotor position sensor is generally used. In Fig.2 a simplified phasor diagram of a load-commutated synchronous motor is presented. The phasor diagram has been drawn using standard notations (X_d and X_q for direct-axis and quadrature-axis synchronous reactances, β for internal electrical angle) neglecting the winding resistance and commutation overlapping effect. In a natural commutation process, the current always leads the voltage and the machine power factor $cos\varphi^{(1)}$ is determined by the phase angle between the inverter triggering pulses and the machine voltage [Bos86].

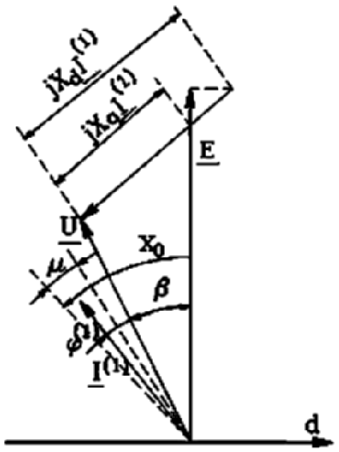

Fig. 2: The simplified phasor diagram of a synchronous motor with load commutation

The commutation angle, μ, is a function of commutation reactance X_c . At commutation limit (with negligible margin angle of commutation) the critical value of μ can be given as

$$\cos \mu_k = 1 - \frac{\pi}{3} \frac{\nu X_c}{U} I^{(1)}, \tag{1}$$

where ν is the frequency expressed in per-unit value, $I^{(1)}$ the r.m.s. (root mean squared) value of the fundamental wave of armature current and U the armature voltage.

Also, the commutation reactance can be calculated in terms of subtransient reactances $X_d^{"}$ and $X_q^{"}$ and the leading angle of commutation x_0, as follows:

A Finite Element two-dimensional analysis can be performed due to FLUX2D's unique features in simulating motion and allowing input from external electric circuits.

By maximizing the average torque calculated from the field analysis, the firing instants of the involved inverter thyristors can be determined.

The whole control imposes the leading angle x_0 determining the thyristors ignition instants with respect to the zero crossing instants of the electromotive force E. The

leading angle variation has the same meaning as the shift of brushes from the neutral axis in a direct current motor.

2.1 Static torque analysis using FLUX2D

In order to calculate the static torque with FLUX2D, a conventional circuit analysis method is used, to assemble the magnetic potential equations together with the current and voltage equations for each conductor. Non-linear functions like flux linkage-current relations are taken into account.
The nonlinear system is iteratively solved using the Newton-Raphson algorithm exploiting a conjugate gradient method to solve the intermediate linear systems.
The characteristics of the analyzed laboratory-used synchronous machine are: P_N = 3.2 kW, U_N = 220 V, 4 salient poles, in rotor: 27 slots, 198 turns/phase. The discretisation frame applied to the transverse section of the synchronous machine is shown in Fig.3.
Due to the fractional slot number (per pole and phase), (q = 9/4) the entire motor must be modeled. The discretisation frame contains 7675 triangular elements (second order) and 15405 nodes.
The static torque generated by two stator phases connected in series and powered with a constant current offers sufficient information to design a suitable current control strategy [TLW96]. This will be explained next.
First, energizing the same two rotor windings ($A-X$ and $B-Y$) connected in series, the static torque was computed for position angle (θ) values spaced at 15 electrical degrees, for a complete rotation of the rotor. The resulting curve of static torque T_{st} = $f(\theta)$ shows a quasi-sinusoidal variation [MK99].
Next, the positions corresponding to the maximum values of the static torque were quantisized in terms of the leading angle x_0 (as example, for x_0 = 60 electrical degrees the first maximum value of the static torque was obtained for a position angle θ = - 30 electrical degrees).

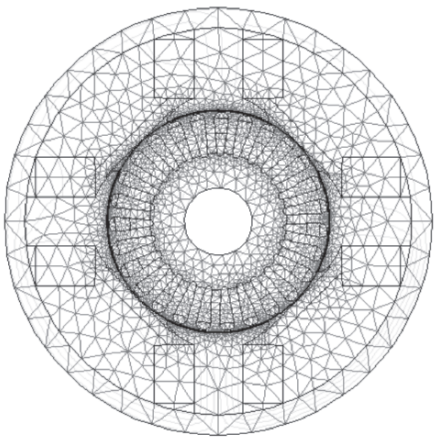

Fig. 3: Discretisation frame applied to the magnetic circuit of the synchronous motor

A magnetostatic simulation in FLUX2D was applied to the circuit structure of Fig.4. The *on* and *off* states of each thyristor (T_1 to T_6) are modeled using a resistance with a low value (1 mΩ for *on* state) or high value (100 kΩ for *off* state).

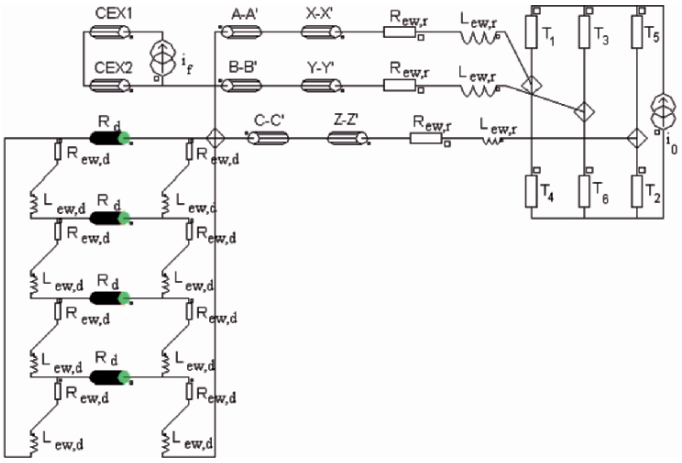

Fig. 4: Structure of the complete circuit for static torque simulation

The supply of the inverter is ensured by a direct current source (value of d.c. link current) i_0.
Each rotor winding is modeled by two stranded conductors (e.g. $A-A'$ and $X-X'$) plus a resistance and a inductance (lumped parameters). The resistance and inductance represent the end turns of winding which are not part of the finite element domain. The values used for modeling the end winding resistance and inductance are 0.1Ω and 1mH, respectively. The damper winding was modeled by four identical circuits, parallel-connected, each composed by a solid conductor resistance and end winding resistances ($R_{ew,d} = 2.87 \times 10^{-6}\Omega$) and inductances ($L_{ew,d} = 0.174mH$).
The field winding circuit is modeled by two stranded conductors (CEX1 and CEX2) and a direct current source (value of field current) i_f.
The obtained variation of maximized static torque is shown in Fig.5, for per-unit (p.u.) values of field current (i_f = 1.52) and constant d.c. link current (i_0 = 0.81) [MK99].
Now, the switching moments of the inverter thyristors, can be determined; depending on the rotor position, the thyristors are turned on and off, for each conduction sequence (60 electrical degrees rotation), to produce a maximum average torque.

2.2 Simulation of the Standstill Frequency Response test

The Standstill Frequency Response test (SSFR) is carried out at standstill and consist in obtaining the Bode diagram for the operational inductance (in direct and quadrature axis) by measuring the armature voltage and current in a range of frequencies [NFC97].
The Finite Element simulation of the Standstill Frequency Response test (SSFR) was carried out by using FLUX2D in linear, quasi-static mode, with coupling to circuit

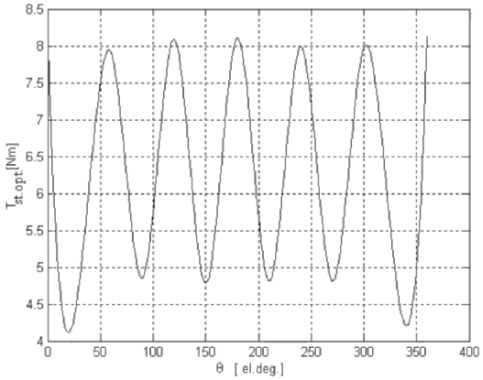

Fig. 5: The maximized static torque

equations. This approach allows to check the operating parameters (inductances and time constants) of a synchronous machine and to compare the simulated values of parameters with those obtained from the short-circuit and SSFR tests.
The circuit structure is shown in Fig.6, with the same notations as in Fig.4.

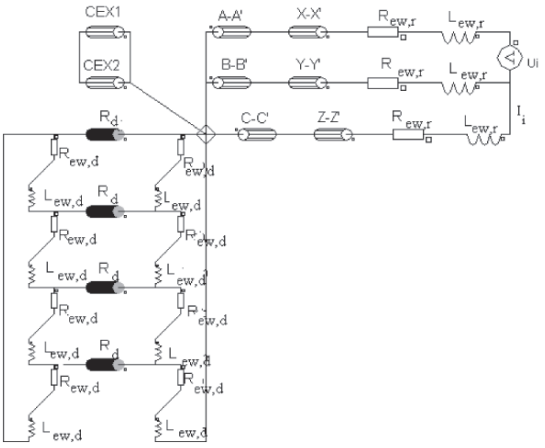

Fig. 6: Structure of the circuit for SSFR test simulation

The sinusoidal a.c. (alternating current) source of tension used in the armature circuit has the value: U_i = 31 mV and the simulation was carried out in a frequency range from 10 mHz to 1000 Hz.
The d-axis operational inductance was calculated by the following relation:

$$L_d(j\omega) = \frac{Z_d(j\omega) - R_a}{j\omega}, \tag{2}$$

with R_a - the armature resistance, $\omega = 2\pi f$, and:

$$Z_d(j\omega) = \frac{2}{3}\frac{U_i(j\omega)}{I_i(j\omega)} \tag{3}$$

The complex d-axis operational inductance depends on the applied frequency of the source. By studying the Bode plot of the amplitude, we can extrapolate linearly this to f = 0, (giving the direct-axis synchronous inductance L_d) and to f = 1000Hz, (giving the direct-axis subtransient inductance, $L_d^{"}$).

3 Results

3.1 Static torque analysis

For unsymmetrical supply (two-phase, without correlation with the rotor position) the flux lines shows a non-uniform distribution (Fig.7).

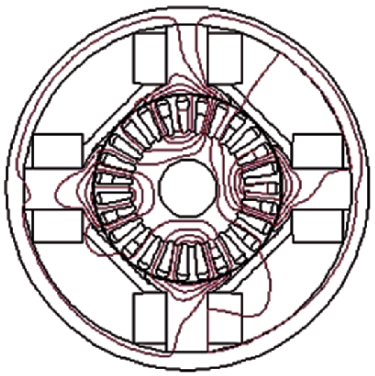

Fig. 7: Flux lines for one rotor position (unoptimized)

For optimized control (two-phase supply, correlated with the rotor position), flux lines becomes much more uniform (Fig.8).
Due to the fractional number of slots per pole and phase the harmonic content of electromotive forces is very small. Consequently, the electromagnetic torque is less affected by non-linearities due to the inverter operation.
For this control optimization was investigated for two cases of a synchronous motor: one with and one without damper winding. The difference between the maximum static torque for the two cases is quite small: $T_{st} = 8.138Nm$ - with damper winding and $T_{st} = 8.0Nm$ - without damper winding [MBM98].
By compensating variations of the current harmonics and by the reduction of overlapping commutation angle, the damper winding acts in reduction of the power factor angle, $\varphi^{(1)}$, thus determining an increase in the overload capability of the motor.
The copper damper winding takes over a part of the imposed magnetomotive force and thus reduces iron losses. The reduction becomes most notable after applying the optimization strategy.
As stated in [MK99], the static torque maximization allows for the correlation between the rotor position angle, θ, and the leading angle x_0 for the firing instants

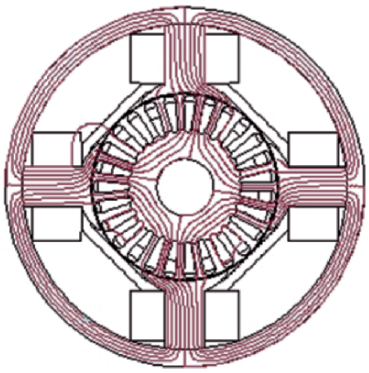

Fig. 8: Flux lines for one rotor position (optimized)

of every inverter thyristor. For example, for an arbitrary value of the leading angle $x_0 \in (0, \pi/2)$ rad., the rotor position angle has the value: $\theta = \pi/2 - x_0$ at the moment when the thyristor T_6 commutates with T_2.

3.2 Simulation of the SSFR test

By simulating the problem of the SSFR test with FLUX2D, for input voltage $U_i = 31mV$, a synchronous inductance $L_d = 34.385mH$ and a subtransient inductance, $L_d^{"} = 4.87mH$, were obtained. These values are in good agreement with experimental ones ($L_d = 36mH$, respectively, $L_d^{"} = 5.4mH$).
For an increased value of $U_i (U_i = 12.4V)$ the saturated values were calculated as well: $L_{d,sat} = 31.4mH$ and $L_{d,sat}^{"} \cong L_d^{"}$.
Also, for a configuration without a damper winding, an increased value of the sub-transient inductance, $L_d^{"} = 5.67mH$ was obtained.
The simulation of the SSFR test was used, also, for computing the q-axis synchronous parameters: the synchronous q-axis inductance, L_q, and the sub-transient q-axis inductance, $L_q^{"}$.
The computed results of the machine parameters are compared to values obtained from experimental determinations. The results, expressed in per-unit values, are presented in Table 1.

Table 1: Parameters comparison

Method	l_d	l_q	$l_d^{'}$	$l_d^{"}$	$l_q^{"}$
Experimental	1.10	0.75	0.38	0.16	0.22
Computation FLUX2D	1.10	0.73	0.35	-	-
Simulation SSFR test	1.05	0.68	-	0.15	0.28

One can observe that the simulation of SSFR test gives satisfactory results, especially in the cases where the skin effect should be taken into account [MBM98].

4 Conclusions

For the synchronous motor studied, the harmonic content of emf's is very small due to the fractional number of slots per pole and phase. Consequently, the electromagnetic torque is less affected by non-linearities due to the inverter operation.
Maximum torque per unit current control strategy is the most widely studied approach in practice. For a given torque, this control strategy minimizes the current; thus, copper losses are minimized in the process.
An accurate determination of the parameters of synchronous machines at the design stage is very important to design engineers, allowing the determination of appropriate materials for machine manufactures by predicting electrical and mechanical overloads during transients.
The Finite Element analysis validates the parameters and evidentiates the need to consider the sub-subtransient reactances due to the skin effect.
By the Standstill Frequency Response test (SSFR) simulation using FLUX2D one can replace different tests performed by the manufacturer, making this tool useful for the design optimization of machines.

References

[FLU05] FLUX2D, version 9.2: Finite element software for electromagnetic applications; CEDRAT, France (2005)
[Bos86] Bose, B.K.: Power Electronics and AC Drives, Prentice-Hall (1996)
[TLW96] Taghezout, D., Lombard, P., Wendling, P.: Finite element prediction of a brushless DC motors dynamic behavior. In: Proc. Intelligent Motions Systems, pp. 59-67 (1996)
[MK99] Manoliu, V. Kisck, D.O: Modelling and simulation of self-controlled synchronous motor considering saturation. In: Proc. of Intern. Symp.ELECTROMOTION99, Patras, Greece, vol. 1, pp. 97-100 (1999)
[NFC97] Nabeta, S. Y., Foggia, A., Coulomb, J.-L., Reyne, G.: Finite element analysis of the skin-effect in damper bars of a synchronous machine. In: IEEE Transactions on Magnetics, vol. 33, no. 2, pp. 2065-2068 (1997)
[MBM98] Manoliu, V., Bl, C., Melcescu, L.: Effects of damper windings on the performances of self-controlled synchronous motor. In: Proc. of Intern. Symp. SPEEDAM98, Sorrento, Italy, pp. P5-57 - P5-61 (1998)